



Chinese Society of Aeronautics and Astronautics
& Beihang University

Chinese Journal of Aeronautics

cja@buaa.edu.cn
www.sciencedirect.com



Microstructure and mechanical properties of hybrid fabricated 1Cr12Ni2WMoVNb steel by laser melting deposition

Wang Yudai, Tang Haibo, Fang Yanli, Wang Huaming *

Engineering Research Center of Ministry of Education on Laser Direct Manufacturing for Large Metallic Components, School of Materials Science and Engineering, Beihang University, Beijing 100191, China

Received 1 December 2011; revised 20 March 2012; accepted 16 April 2012
Available online 7 March 2013

KEYWORDS

Heat affected zone;
Laser melting deposition;
Martensitic stainless steel;
Mechanical properties;
Metallic material;
Solid phase transformation

Abstract Laser melting deposition was carried out to deposit a 1Cr12Ni2WMoVNb steel bar on a wrought bar of same material. Room-temperature tensile properties of the hybrid fabricated 1Cr12Ni2WMoVNb steel sample were evaluated, and microstructure, fracture surface morphology, and hardness profile were analyzed by an optical microscope (OM), a scanning electron microscope (SEM), and a hardness tester. Results show that the hybrid fabricated 1Cr12Ni2WMoVNb steel sample consists of laser deposited zone, wrought substrate zone, and heat affected zone (HAZ) of the wrought substrate. The laser deposited zone has coarse columnar prior austenite grains and fine well-aligned dendritic structure, while the HAZ of the wrought substrate has equiaxed prior austenite grains which are notably finer than those in the wrought substrate zone. Besides, austenitic transformation mechanism of the HAZ of the wrought substrate is different from that of the laser deposited zone during the reheating period of the laser deposition, which determines the different prior austenite grain morphologies of the two zones. Microhardness values of both the laser deposited zone and the HAZ of the wrought substrate are higher than that of the wrought substrate zone. Tensile properties of the hybrid fabricated 1Cr12Ni2WMoVNb steel sample are comparable to those of the wrought bar, and fracture occurs in the wrought substrate zone during the tensile test.

© 2013 Production and hosting by Elsevier Ltd. on behalf of CSAA & BUAA.
Open access under [CC BY-NC-ND license](#).

1. Introduction

Martensitic stainless steel 1Cr12Ni2WMoVNb (GX-8) with excellent mechanical properties and moderate corrosion resistance is widely used as compressor blade, disc, shaft, etc. in gas and steam turbines.¹

Laser melting deposition (LMD) is a rapid solidification-based near-net-shaping technology for building fully dense components through layer-by-layer melting deposition of metal

* Corresponding author. Tel.: +86 10 82317102.
E-mail addresses: wyudai@yahoo.com.cn (Y. Wang), wanghm@buaa.edu.cn (H. Wang).

Peer review under responsibility of Editorial Committee of CJA.



Production and hosting by Elsevier

powders.²⁻⁸ This technology has the advantage of producing complex components of difficult-to-process materials by contrast with conventional manufacturing routes like forging or casting. Moreover, laser deposited metal parts have excellent mechanical properties which are usually comparable or even superior to forged materials due to fine rapidly solidified microstructures. Laser deposited titanium alloy components have been successfully used as aircraft load-bearing structural components.^{9,10}

Special features can be added to local areas of a simplified forging or casting by LMD in order to obtain a large and complex final part.^{11,12} This process is a hybrid fabrication based on LMD. Conventional manufacturing routes like forging or casting are suitable for making large and regular parts, while LMD has significant process flexibility on producing complex parts. Combining the advantages of both conventional manufacturing routes and laser melting deposition, the hybrid fabrication can make substantial savings in the amount of materials and time required to make the final parts.¹¹ Another application for LMD is laser repairing or rebuilding worn components, which can effectively extend service lives of components and reduce costs.¹³⁻¹⁸ One common concern for hybrid fabrication and laser repair is the mechanical properties of the final parts, which are expected to be at least equal to those of the substrate materials. The mechanical properties of the hybrid fabricated or laser repaired final parts are dependent on microstructure of the parts especially in the heat affected zone (HAZ) of the substrate materials. Repaired parts using conventional welding techniques such as tungsten-arc inert-gas (TIG) welding or metal-inert gas (MIG) welding usually have high thermal stresses and wide HAZ with coarsening grains and microstructure due to high heat input, which obviously deteriorates the mechanical properties of the repaired parts.¹⁶⁻¹⁸ By contrast with TIG welding and MIG welding, small HAZ with fine microstructure and high mechanical properties could be obtained through hybrid fabrication or laser repair due to low heat input. With regard to martensitic stainless steels, relevant papers on microstructure and mechanical properties are very limited. Xue et al. investigated microstructure and tensile properties of laser repaired 1Cr12Ni3MoVN steel casting, and found that fracture occurred from casting substrate during tensile tests.¹⁹ To gain a further understanding on microstructure and mechanical properties of hybrid fabricated or laser repaired martensitic stainless steels, more work needs to be done.

In the present study, LMD was carried out to deposit a 1Cr12Ni2WMoVNb steel bar on a wrought bar of same material. Microstructure, effect of thermal cycles during the laser deposition on prior austenite grain morphologies, and tensile properties of the hybrid fabricated steel were investigated.

2. Experimental procedure

Plasma rotation electrode processing 1Cr12Ni2WMoVNb steel powders with a particle size ranging from 75 to 250 μm were selected as the raw materials. Chemical composition (wt.%) of the powders was C 0.16, Cr 11.76, Ni 2.06, W 0.82, Mo 0.98, V 0.25, Nb 0.23, Si 0.33, Mn 0.16, S 0.0025, P 0.016, Fe balance. The substrate material was a 1Cr12Ni2WMoVNb steel wrought bar with dimensions of $\text{O}55\text{ mm} \times 30\text{ mm}$. The wrought bar was in a standard quenched-and-tempered state (1150 $^{\circ}\text{C}$

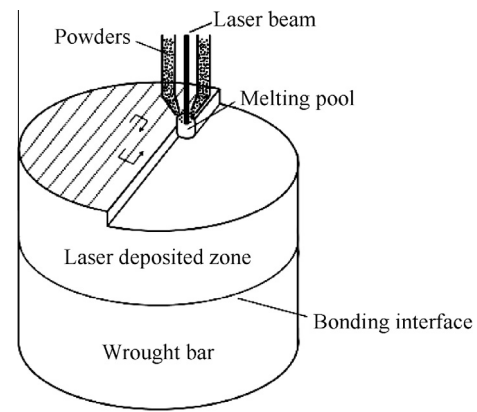


Fig. 1 Schematic illustration of the laser deposition process for the hybrid fabricated 1Cr12Ni2WMoVNb steel sample.

solution treatment followed by oil quenching + 580 $^{\circ}\text{C}$ tempering). Before laser deposition, the wrought bar was sandblasted. LMD was carried out using a LMD system equipped with a GS-TFL-8000 CO_2 laser (maximum output power 8 kW), a BSF-2 powder feeder together with a co-axial powder delivery nozzle, a HNC-21M computer numerical control (CNC) multi-axis motion system, and an argon-purged processing chamber with oxygen content less than 100×10^{-6} . A 1Cr12Ni2WMoVNb steel bar sample with dimensions of approximately $\text{O}55\text{ mm} \times 30\text{ mm}$ was laser deposited on the wrought substrate. The processing parameters were as follows: laser beam power 4.5–5.0 kW, scanning speed 4–5 mm/s, beam diameter 5 mm, powder delivery rate 6.5–7.5 g/min, overlap ratio 30%–50%. The scanning mode was to-and-fro scanning. A schematic illustration of the laser deposition process for the hybrid fabricated 1Cr12Ni2WMoVNb steel sample was shown in Fig. 1. The newly laser deposited sample was tempered at 580 $^{\circ}\text{C}$ for 2 h in order to eliminate residual stresses and obtain a tempered microstructure.

Metallographic samples were prepared using standard practices and examined by an optical microscope (OM). The etchant is a mixture of 4 g picric acid, 5 ml hydrochloric acid, and 100 ml ethanol. Microhardness profile of the hybrid fabricated sample was measured by using a HXZ-1000 semi-automatic Vicker tester with a test load of 500 g and a dwell time of

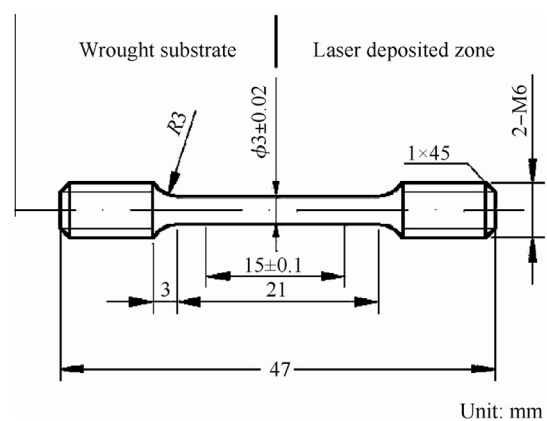


Fig. 2 Geometric shape and size of a room-temperature tensile specimen.

10 s. Room-temperature tensile tests based on the standard of ISO 6892: 1998 were performed on 3 mm diameter round specimens with 15 mm gauge length and 47 mm total length. The principle axis of the specimens was parallel to the deposition direction (Z direction), and the bonding interface between the laser deposited zone and the wrought substrate (melting line) was in the middle of the specimens, as shown in Fig. 2. The fracture surfaces were examined by a scanning electron microscope (SEM).

3. Results and discussion

3.1. Microstructure

Fig. 3 shows microstructure of the hybrid fabricated 1Cr12Ni2WMoVNb steel sample. There is a good metallurgical bonding between the laser deposited zone and the wrought substrate without metallurgical defects such as gas porosities, lack-of-fusion porosities, etc. The hybrid fabricated 1Cr12Ni2WMoVNb steel sample consists of laser deposited zone, wrought substrate zone, and heat affected zone (HAZ) of the wrought substrate.

Fig. 4 shows microstructure of the laser deposited zone and the wrought substrate zone. The laser deposited zone has coarse columnar prior austenite grains, and the width of the columnar grains exceeds 100 μm . The columnar prior austenite grains are composed of many fine well-aligned dendrites with a primary arm spacing of 11–15 μm . Microstructure of the laser deposited zone is fine tempered sorbite. The wrought substrate zone has equiaxed grains, and the average grain size is 27.9 μm . Microstructure of the wrought substrate is typical tempered sorbite, which is much coarser than that of the laser deposited zone.

Microstructure of the HAZ of the wrought substrate has a gradual transition along the depth direction, as shown in Fig. 5(a), which is associated with the thermal cycles during la-

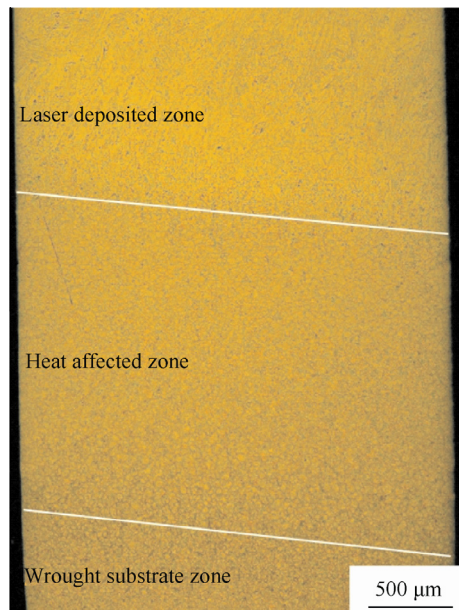


Fig. 3 Microstructure of the hybrid fabricated 1Cr12Ni2W-MoVNb steel sample.

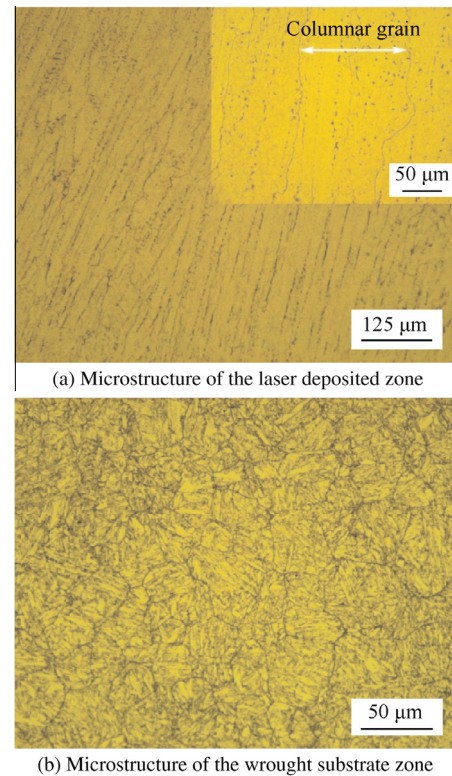


Fig. 4 Microstructure of the laser deposited zone and the wrought substrate zone.

ser deposition. Here, the depth is defined as the distance from the melting line. Along the depth direction, the maximum reheating temperature decreases gradually, and the HAZ of the wrought substrate can be divided into three zones: sufficiently quenched zone, insufficiently quenched zone, and tempered zone. In the sufficiently quenched zone, the reheating temperature is above A_{c3} (the temperature at which ferrite-to-austenite transformation is completed during heating), so the wrought substrate transforms from tempered sorbite to austenite during the reheating period and austenite transforms to martensite during the subsequent cooling process. The sufficiently quenched zone has fine equiaxed prior austenite grains, and the grain size decreases with the increase of the depth. Fig. 5(b) shows the prior austenite grain morphology of the sufficiently quenched zone close to the melting line. The average grain size is 21.4 μm , which is finer than that of the wrought substrate zone. Fig. 5(c) shows the prior austenite grain morphology of the sufficiently quenched zone away from the melting line. The average grain size becomes much finer, which is less than 10 μm . In the insufficiently quenched zone, the reheating temperature is between A_{c1} (the temperature at which ferrite-to-austenite transformation begins during heating) and A_{c3} , so the wrought substrate is partially austenitized during the reheating period and forms a mixed microstructure of martensite and tempered sorbite during the subsequent cooling process (Fig. 5(d)). In the tempered zone, the reheating temperature is below A_{c1} , so microstructure of the wrought substrate has no obvious change.

During the laser deposition process, the substrate material and the previously deposited zone suffer heat treatment from the moving melt pool. As the scanning mode is to-and-fro cyclic scanning in track-by-track and layer-by-layer manners, the

wrought substrate and the previously deposited zone undergo cyclic thermal fluctuations. Reheating rate and subsequent cooling rate are very fast, meanwhile, the cyclic thermal fluctuations get weaker and weaker with the increase of distance from the layer being deposited.²⁰ The thermal cycles during the laser deposition can induce complex solid phase transformations and diverse microstructure. During the deposition of the first layer, a certain depth of the wrought substrate is austenitized and the austenitization depth is about 1–2 mm (Fig. 3). Due to the rapid reheating rate, austenite nucleation rate is high, and the wrought substrate is subsequently cooled down before austenite grains grow up. Therefore, compared with the wrought substrate zone (without heat treatment), the HAZ of the wrought substrate (even the HAZ close to the melting line) has notably finer grains. With the increase of the depth, the maximum austenitization temperature declines, and the austenite grains get finer gradually, as shown in Fig. 5. During the subsequent cooling process, austenite transforms to martensite. As a result of the rapid cooling rate and the fine austenite grains, the martensite is also very fine. When the second or more layers are deposited, the maximum reheating temperature of the HAZ of the wrought substrate declines below A_{c1} , so the martensite is slightly tempered.

As mentioned above, prior austenite grain refinement occurs in the HAZ of the wrought substrate during the thermal cycles. However, instead of forming fine equiaxed prior austenite grains, the laser deposited zone remains coarse columnar grain morphology despite suffering the similar thermal cycles. This indicates that the laser deposited zone and the HAZ of the wrought substrate have different austenite transformation mechanisms during the thermal cycles. Due to high temperature gradient and rapid solidification cooling rate, the newly laser deposited 1Cr12Ni2WMoVNb steel forms columnar austenite grains, and austenite subsequently transforms to martensite. When the next layer is deposited, the previous layer is re-austenitized. For high alloy steels such as 1Cr12Ni2WMoVNb steel, if martensite or tempered martensite is reheated very rapidly above A_{c3} to transform to austenite, the new austenite grains will inherit or recover the shape, size, and orientation of the original austenite grains.²¹ In other words, the new austenite grains will remain columnar grain morphology during the thermal cycles. On the other hand, the original microstructure of the wrought substrate is tempered sorbite. When martensite is tempered at high temperature to form tempered sorbite, the orientation relationship between prior martensite laths could partially disappear. As a result, when tempered sorbite is re-austenitized, new austenite grains form fine equiaxed grains instead of inheriting or recovering the original coarse equiaxed grains. According to the analysis above, the original microstructures of the laser deposited zone and the HAZ of the wrought substrate are martensite and tempered sorbite, respectively, and have different austenite transformation mechanisms during the thermal cycles, which determine the different austenite grain morphologies of the two zones. Provided that the newly laser deposited layer is immediately tempered to form tempered sorbite through some method, then the layer will be re-austenitized to form fine equiaxed grains when the next layer is deposited. By this method, the laser deposited zone is expected to have fine equiaxed grains instead of coarse columnar grains.

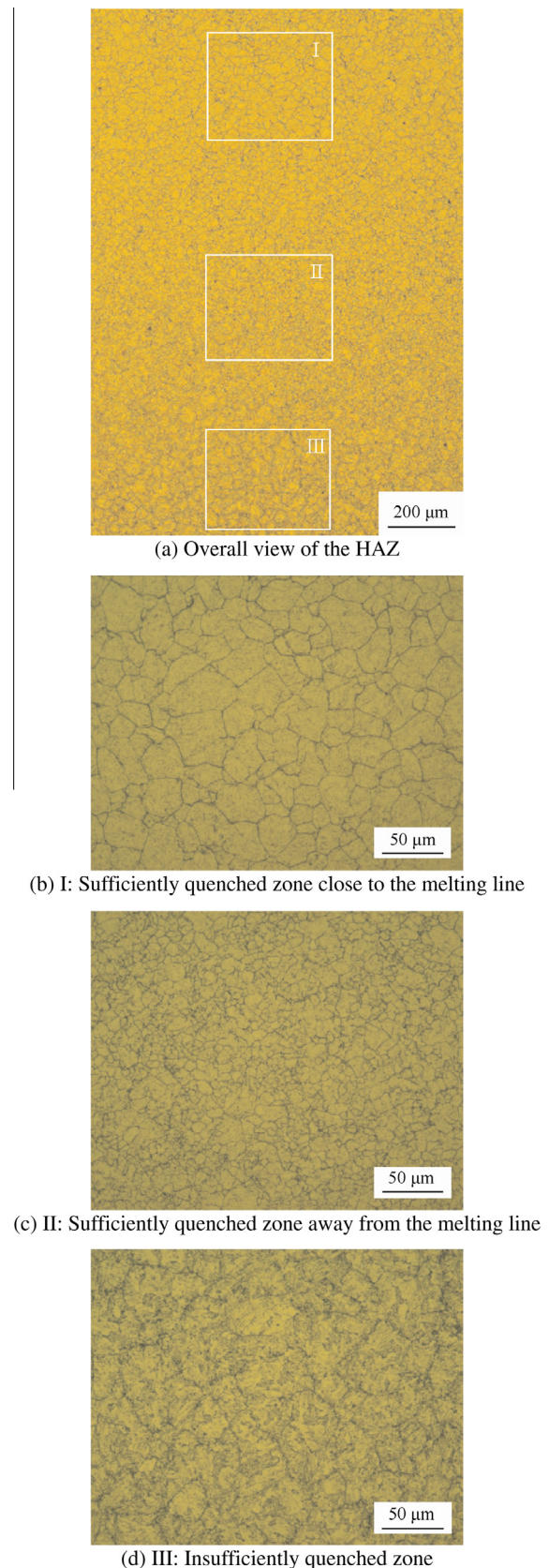


Fig. 5 Microstructure of the HAZ of the wrought substrate.

3.2. Microhardness profile

Fig. 6 shows microhardness profile of the hybrid fabricated 1Cr12Ni2WMoVNb steel sample (test load is 500 g and load time is 10 s). Microhardness of the laser deposited zone is about 50 HV higher than that of the wrought substrate zone. Microhardness of the HAZ of the wrought substrate close to the melting line is slightly higher than that of the laser deposited zone. With the increase of the depth, microhardness of the HAZ of the wrought substrate keeps nearly constant at the beginning and then declines gradually to the level of the wrought substrate zone.

The laser deposited zone has a fine well-aligned dendritic structure and fine tempered sorbite, which helps to improve the microhardness. The HAZ of the wrought substrate has notably finer equiaxed prior austenite grains and microstructure than the wrought substrate zone, thus microhardness of the HAZ of the wrought substrate is higher than that of the wrought substrate zone. The HAZ of the wrought substrate close to the melting line (the sufficiently quenched zone) is sufficiently re-austenitized during the thermal cycles, and microhardness of the zone keeps nearly constant. With the increase of the depth, austenitization is insufficient, and consequently microhardness declines gradually to the level of the wrought substrate zone.

3.3. Room-temperature tensile properties

Room-temperature tensile properties of the hybrid fabricated 1Cr12Ni2WMoVNb steel sample are comparable to the wrought bar, as shown in Table 1. Average ultimate tensile strength of the hybrid fabricated steel component is 1207 MPa. Moreover, the tensile properties of the laser melting deposited 1Cr12Ni2WMoVNb steel are also listed in Table 1 for the purpose of comparison. As can be seen, the ultimate tensile strength of the laser melting deposited steel is slightly higher than those of the wrought bar and the hybrid fabricated

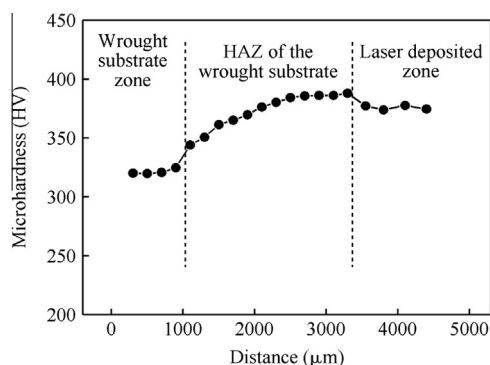


Fig. 6 Microhardness profile of the hybrid fabricated 1Cr12Ni2WMoVNb steel sample.

steel sample. Fig. 7 shows fracture surface of a tensile specimen of the hybrid fabricated 1Cr12Ni2WMoVNb steel sample. No metallurgical defects are found. The fracture surface consists of fibrous zone, crack propagation zone, and shear rupture zone. There are lots of secondary cracks in the fibrous zone.

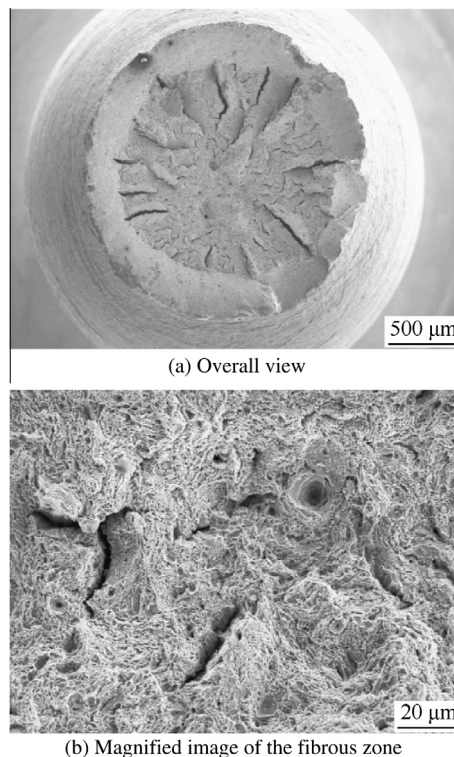


Fig. 7 Fracture surface of a tensile specimen of the hybrid fabricated 1Cr12Ni2WMoVNb steel sample.

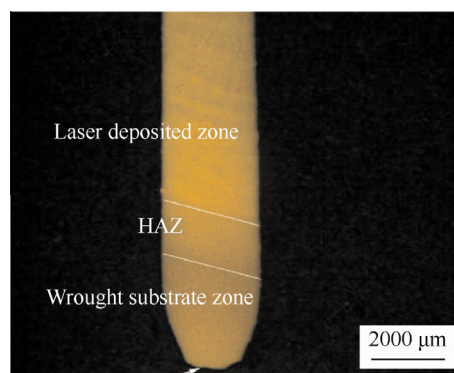


Fig. 8 Cross-sectional morphology of a tensile specimen of the hybrid fabricated 1Cr12Ni2WMoVNb steel sample (fracture surface is indicated by the white arrow).

Table 1 Room-temperature tensile properties of the hybrid fabricated 1Cr12Ni2WMoVNb steel sample.

Materials	σ_b (MPa)	$\sigma_{0.2}$ (MPa)	δ (%)	ψ (%)
Hybrid fabricated 1Cr12Ni2WMoVNb steel sample	1207 ± 5.8	1027 ± 5.8	14.0 ± 1.73	59.8 ± 3.82
Wrought bar (1150 °C, oil-quenched + 580 °C, air-cooled) ¹	1199	1041	17.2	67.2
Laser melting deposited 1Cr12Ni2WMoVNb steel (580 °C, air-cooled) ²²	1223 ± 20.8		7.7 ± 0.58	38.7 ± 8.50

and crack propagation zone. Magnified image of the fibrous zone shows a dimpled morphology.

Fig. 8 shows cross-sectional morphology of a tensile specimen of the hybrid fabricated 1Cr12Ni2WMoVNb steel sample. The fracture site is in the wrought substrate zone away from the HAZ of the wrought substrate. As mentioned previously, the laser deposited zone and the HAZ of the wrought substrate zone have finer microstructure and higher microhardness than the wrought substrate, so tensile properties of the two zones are superior to the wrought substrate zone accordingly.

4. Conclusions

- (1) LMD was carried out to deposit a 1Cr12Ni2WMoVNb steel bar on a wrought bar of same material. There is a good metallurgical bonding between the laser deposited zone and the wrought substrate. Grain refinement occurs in the HAZ of the wrought substrate during the thermal cycles.
- (2) The laser deposited zone and the HAZ of the wrought substrate have different austenite transformation mechanisms during the thermal cycles, which determine different prior austenite grain morphologies of the two zones.
- (3) Microhardness of the laser deposited zone and the HAZ of the wrought substrate is higher than that of the wrought substrate zone. Microhardness of the HAZ of the wrought substrate close to the melting line is slightly higher than that of the laser deposited zone. With the increase of the distance from the melting line, microhardness of the HAZ of the wrought substrate keeps nearly constant at the beginning and then declines gradually to the level of the wrought substrate zone.
- (4) Room-temperature tensile properties of the hybrid fabricated 1Cr12Ni2WMoVNb steel sample are comparable to those of the wrought bar. Fracture occurs in the wrought substrate zone during the tensile test.

Acknowledgement

The authors acknowledge financial supports from the Cheung Kong Scholars and Innovative Research Team Program of Ministry of Education (No. IRT0805) and the National Basic Research Program of China (No. 2010CB731705).

References

1. Yan MG, Liu DP, Shi CX. *China aeronautical materials handbook, vol. 1: Structural and stainless steel*. Beijing: China Standard Press; 1988, 677–697 [Chinese].
2. Lewis GK, Schlienger E. Practical considerations and capabilities for laser assisted direct metal deposition. *Mater Des* 2000;**21**(4):417–23.
3. Mazumder J, Dutta D, Kikuchi N, Ghosha A. Closed loop direct metal deposition: art to part. *Opt Lasers Eng* 2000;**34**(4–6):397–414.
4. Wu L, Liang J, Mei J, Mitchell C, Goodwin PS, Voice W. Microstructures of laser-deposited Ti-6Al-4V. *Mater Des* 2004;**25**(2): 137–44.
5. Zhang Y, Xi M, Gao S, Shi LK. Characterization of laser direct deposited metallic parts. *J Mater Process Tech* 2003;**142**(2):582–5.
6. Feng L, Huang W, Lin X, Yang HO, Li YM, Yang J. Laser multi-layer cladding experiment on the DD3 single crystal using FGH95 powder: investigation on the microstructure of single crystal cladding layer. *Chin J Aeronaut* 2002;**15**(2):121–7.
7. Wang HM. Research progress on laser surface modifications of metallic materials and laser rapid forming of high performance metallic components. *Acta Aeronaut Astronaut Sin* 2002;**23**(5):473–8.
8. He R, Wang H. HCF properties of laser deposited Ti-6Al-2Zr-Mo-V alloy. *Acta Aeronaut Astronaut Sin* 2010;**31**(7):1488–93 [Chinese].
9. Santos EC, Shiomi M, Osakada K, Laoui T. Rapid manufacturing of metal components by laser forming. *Int J Mach Tools Manuf* 2006;**46**(12–13):1459–68.
10. Wang HM, Zhang SQ. Progress and challenges of laser direct manufacturing of large titanium structural components. *Chin J Lasers* 2009;**36**(12):3204–9 [Chinese].
11. Mudge RP, Wald NR. Laser engineered net shaping advances additive manufacturing and repair. *Weld J* 2007;**86**(1):44–8.
12. Xue L. Direct manufacturing of net-shape functional components by laser consolidation process. *Chin J Lasers* 2009;**36**(12):3179–91.
13. Gäumann M, Bezençon C, Canalis P, Kurz W. Single-crystal laser deposition of superalloys: processing- microstructure maps. *Acta Mater* 2001;**49**(6):1051–62.
14. Li L. Repair of directionally solidified superalloy GTD-111 by laser engineered net shaping. *J Mater Sci* 2006;**41**(23):7886–93.
15. Song JL, Deng QL, Chen CY, Hu DJ, Li YT. Rebuilding of metal components with laser cladding forming. *Appl Surf Sci* 2006;**252**(22):7934–40.
16. Xue L, Huang WD, Chen J, Lin X. Application of laser forming repair technology on the aerial castings. *Foundry Technol* 2008;**29**(3):391–4 [Chinese].
17. Sexton L, Lavin S, Byrne G, Kennedy A. Laser cladding of aerospace materials. *J Mater Process Technol* 2002;**122**(1):63–8.
18. Pinkerton AJ, Wang W, Li L. Component repair using laser direct metal deposition. *Proce Inst Mech Engr. Part B: J Eng Manuf* 2008;**222**(7):827–36.
19. Xue L, Lu PH, Chen J, Lin X, Huang WD. Study on microstructure and mechanical properties of laser repaired 1Cr12Ni3MoVN alloy. *Chin J Lasers* 2010;**37**(3):887–90 [Chinese].
20. Griffith ML, Schlienger ME, Harwell LD, Oliver MS, Baldwin MT, Ensz MT. Understanding thermal behavior in the LENS process. *Mater Des* 1999;**20**(2–3):107–13.
21. Zhao NQ, Yang ZG, Feng YL. *Solid phase transformations in alloys*. Changsha: Central South University Press; 2008, 85–91 [Chinese].
22. Wang YD, Tang HB, Fang YL, Wang HM. Microstructure and mechanical properties of laser melting deposited 1Cr12Ni2W-MoVNb steel. *Mater Sci Eng:A* 2010;**527**(18–19):4804–9.

Wang Yudai received his B.S. degree from China University of Mining and Technology (Beijing) in 2006, and now is a Ph.D. candidate in the School of Materials Science and Engineering at Beihang University. His current research interest is laser rapid forming of metallic components.

Wang Huaming is a professor and Ph.D. supervisor in the School of Materials Science and Engineering at Beihang University. His main research interests involve laser materials processing and manufacturing.